RSC Advances

PAPER

View Article Online
View Journal | View Issue

Check for updates

Cite this: *RSC Adv.*, 2025, **15**, 1152

Intramolecular noncovalent C-bonding driven conformational preference in spiroisatin-based *N*-acyl hydrazones†‡

Muhammad Imran Ali, [a] Javid Hussain,[b] Muhammad Usman Anwar, [b] Ahmed Al-Harrasi [c] and Muhammad Moazzam Naseer *[a]

Noncovalent carbon bonding (C-bonding), a recently explored σ-hole interaction, has primarily been characterized through X-ray structural and computational studies. Evidence of C-bonds in solution is scarce, especially in highly polar solvents like DMSO where solvation effects typically overshadow weak non-covalent interactions. In this work, we present three novel spiroisatin-based *N*-acyl hydrazones (**1**–**3**) in which C-bonds play a critical role in stabilizing the *cis* conformation in solution. Despite the steric preference for the NH–amide bond to adopt the *trans* geometry (H–N–C=O ≈ 180°), ^{1}H and ^{13}C NMR spectra of compounds **1** and **2** in DMSO-d_6 reveal a rotameric mixture with a higher percentage of the *cis* conformation (82% and 76%, respectively), attributed to the stability provided by intramolecular C-bonding. Compound **3** also predominantly adopts the *cis* conformation in DMSO but to a lesser extent (60%) than compounds **1** and **2**, due to competing intramolecular hydrogen bonding. Single-crystal X-ray analysis of compounds **1** and **2** confirmed the *cis* conformation, consistent with the solution-state preference. In contrast, compound **3** crystallized in the *trans* form, likely due to intramolecular hydrogen bonding and solid-state packing effects, which reinforce the steric preference for the *trans* geometry. Density functional theory (DFT) calculations corroborated the experimental data, predicting greater stability for the *cis* conformations in compounds **1**, **2**, and **3** in solution. The ability of intramolecular C-bonding to stabilize the *cis* conformation, even in highly polar solvents like DMSO, highlights the broader significance of this interaction in supramolecular chemistry and related fields.

Received 14th November 2024
Accepted 7th January 2025

DOI: 10.1039/d4ra08086f

rsc.li/rsc-advances

Open Access Article. Published on 13 January 2025. Downloaded on 2/14/2026 10:03:16 PM.
This article is licensed under a Creative Commons Attribution-NonCommercial 3.0 Unported Licence.

1. Introduction

Non-covalent interactions are fundamental across chemistry, physics, and biological sciences, playing a key role in maintaining the three-dimensional structures of biomacromolecules such as nucleic acids and proteins, and mediating molecular recognition processes like receptor–ligand binding, enzyme–substrate interactions, and antigen–antibody recognition.[1–3] While well-established interactions such as hydrogen[4] and halogen bonds[5,6] have been extensively characterized, increasing attention has been directed towards weaker non-covalent interactions, particularly in the context of molecular organization in solution (self-assembly)[7] and in the solid state (crystal engineering).[8,9] Interactions such as C–H···O[10,11] and C–H···π[12,13] once considered weak, are now recognized for their importance in stabilizing molecular conformations, promoting crystallization, and influencing selectivity, despite their relatively low energies (3 kcal mol^{-1} for C–H···O[14,15] and 0.8 kcal mol^{-1} for C–H···π[16] compared to stronger hydrogen bonds). These interactions are also considered crucial in processes like protein folding,[17,18] and higher-order molecular assembly.[16] Concludingly, the scientific focus has recently been expanded to unravel the behavior of newly discovered non-covalent interactions such as chalcogen,[19–21] pnicogen,[22–24] aerogen,[25,26] and C-bonding.[27–29] Among these non-covalent σ-hole interactions (a concept originally introduced by Politzer *et al.*[30,31]), C-bonding was first highlighted in 2013 by Mani and Arunan through theoretical calculations on the Ar···propargyl alcohol complex,[32] and later confirmed experimentally by Guru Row and colleagues *via* X-ray charge density analysis.[33] Although C-bonding has been proposed as a significant interaction with broad implications in supramolecular chemistry, research remains limited in elucidating its role in directing structure in chemical and biological sciences.

[a]*Department of Chemistry, Quaid-i-Azam University, Islamabad 45320, Pakistan. E-mail: moazzam@qau.edu.pk*

[b]*Department of Biological Sciences & Chemistry, College of Arts and Sciences, University of Nizwa, Nizwa, Oman*

[c]*Natural and Medical Sciences Research Centre, University of Nizwa, Birkat Almouz 616, Oman*

† Dedicated to Prof. Dr Klaus Jurkschat of TU Dortmund on occasion of his 73rd birthday.

‡ Electronic supplementary information (ESI) available. CCDC 2401916–2401918. For ESI and crystallographic data in CIF or other electronic format see DOI: https://doi.org/10.1039/d4ra08086f

© 2025 The Author(s). Published by the Royal Society of Chemistry

Open Access Article. Published on 13 January 2025. Downloaded on 2/14/2026 10:03:16 PM.
This article is licensed under a Creative Commons Attribution-NonCommercial 3.0 Unported Licence.

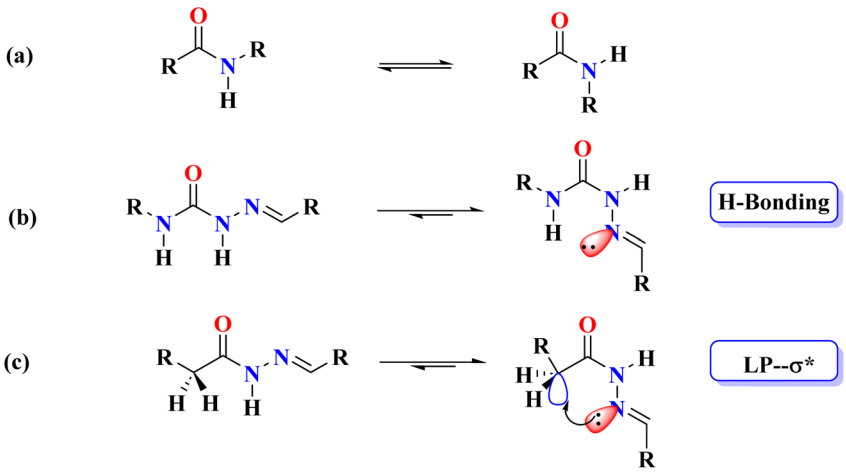

Fig. 1 Showing *trans* (left) and *cis* (right) conformations, (a) amides; (b) semicarbazones; (c) acylhydrazones.

An analysis of protein structures reveals that, with the exception of proline, all-natural amino acids overwhelmingly favor the *trans* isomer (>99.9%) due to steric factors.[34–37] In contrast, semicarbazones and thiosemicarbazones predominantly adopt the *cis* conformation for their amide and thioamide groups, respectively, which is attributed to the presence of intramolecular hydrogen bonding (Fig. 1).[38] This led to the hypothesis that replacing the NH group in semicarbazones with a CH_2 group in acyl hydrazones would result in either a *cis* conformation stabilized by C-bonding or a *trans* conformation in the absence of any intramolecular non-covalent interactions (Fig. 1). Based on this hypothesis, we were the first to demonstrate the role of C-bonding in stabilizing the *cis* conformation in the solid state.[39] Later, Sarma and colleagues extended this concept to solution-phase studies specifically in chloroform using *N*-methyl-*N*,*N*-diacylhydrazines as models.[40] Mooibroek and co-workers, through X-ray diffraction and DFT studies, further demonstrated the application of C-bonds in crystal engineering.[41] Wang *et al.* later provided substantial evidence of the importance of C-bonds in catalysis through NMR spectroscopy.[42] Most notably, Biswal and co-workers underscored the ubiquitous presence of C-bonds in proteins using detailed structural analyses and quantum mechanical calculations to highlight their ubiquity.[43]

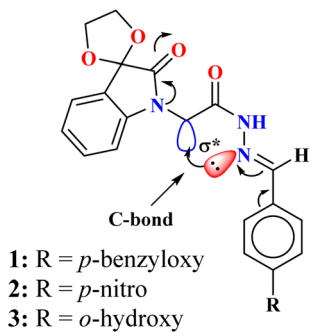

Fig. 2 Novel spiroisatin-based *N*-acyl hydrazones **1**–**3**.

In this study, we report three novel *N*-acyl hydrazones **1**–**3** (Fig. 2) featuring an isatin nucleus, where the nitrogen exhibits increased electronegativity due to lone pair delocalization onto the 2-carbonyl group of the isatin ring. This delocalization enhances the electrophilic character of the adjacent CH_2 group, increasing its potential for non-covalent C-bonding interactions. Thus, the ^1H and ^{13}C NMR spectra of compounds **1**, **2**, and **3** in DMSO-d_6 reveal a rotameric mixture favoring the *cis* conformation in 82%, 76%, and 60% respectively due to intramolecular C-bonding. These findings are further supported by X-ray single-crystal analysis and theoretical calculations. This study not only demonstrates the potential of intramolecular C-bonding to stabilize specific conformations but also lays a foundation for further investigation into the nature of this interaction. These insights may have important implications for crystallography, supramolecular chemistry, and related fields of research.

2. Experimental

2.1. Synthesis of ethyl 2-(2-oxospiro[indoline-3,2′-[1,3]dioxolan]-1-yl)acetate (I)

To a round-bottom flask connected to a water separator (Dean–Stark apparatus), commercially available isatin (1 mmol, 147.13 mg) was added in toluene (30 mL) and allowed to react with ethylene glycol (2 mmol, 124.14 mg, 111.83 μL) in the presence of a catalytic amount of *p*-TsOH. Upon completion of the reaction, the mixture was poured into chilled water. The desired spiroisatin-ketal was extracted with ethyl acetate and recrystallized from ethanol.[44] This purified spiroisatin-ketal (1 mmol, 191.19 mg) was then stirred at room temperature with potassium carbonate (1.20 mmol, 165.85 mg) in DMF (20 mL), and ethyl bromoacetate (1.1 mmol, 183.70 mg, 121.66 μL) was added to it dropwise, and the reaction was allowed to continue for 4 hours. Upon completion, the product was collected *via* solvent extraction and purified through recrystallization from ethanol. The synthesized spiroisatin-based ester **I** was characterized by comparing its melting point.[45,46]

Open Access Article. Published on 13 January 2025. Downloaded on 2/14/2026 10:03:16 PM. This article is licensed under a Creative Commons Attribution-NonCommercial 3.0 Unported Licence.

2.2. Synthesis of 2-(2-oxospiro[indoline-3,2′-[1,3]dioxolan]-1-yl)acetohydrazide (II)

In a round-bottom flask, spiroisatin-based ester **I** (1 mmol, 277.28 mg) was dissolved in ethanol (20 mL), and hydrazine hydrate (3 mmol, 100.12 mg, 97.21 μL) was added to the mixture. The reaction mixture was refluxed with continuous stirring. The resulting hydrazide **II** was collected by filtration, washed, and recrystallized from ethanol.

White solid; yield 90%; R_f 0.3 (EtOAc/*n*-hexane 1 : 1); m.p. 228–229 °C; FT-IR $\bar{\upsilon}$ (cm^{-1}); 3220 (NH_2), 3113 (N–H), 3022 (C_{sp^2}–H), 1738 (C=O, spiroisatin), 1703 (C=O, acetohydrazide), 1274 (C–N, lactam), 1139 (C–O–C).

2.3. General procedure for the synthesis of compounds 1–3

In a round-bottom flask, commercially available aromatic aldehyde (1 mmol) was dissolved in methanol (10 mL). A few drops of acetic acid were added as a catalyst, and the reaction mixture was stirred for 15 minutes. Afterward, spiroisatin-bearing *N*-acetohydrazide **II** (1 mmol, 263.25 mg) was added, and the reaction mixture was refluxed for 6 hours. The resulting compound precipitated out, were collected by filtration, washed, and recrystallized from ethanol to get pure **1–3**.

2.3.1. *N*′-(4-(Benzyloxy)benzylidene)-2-(2-oxospiro[indoline-3,2′-[1,3]dioxolan]-1-yl)acetoh ydrazide (1). White crystals; yield 78%; m.p. 241–242 °C; FT-IR $\bar{\upsilon}$ (cm^{-1}); 3144 (N–H), 3079 (C_{sp^2}–H), 1734 (C=O, spiroisatin), 1678 (C=O, acetohydrazide), 1601 (C=N imine str.), 1245 (C–N, lactam), 1134 (C–O–C); ^{1}H NMR (300 MHz, DMSO-d_6) δ; (*cis*, 82%) 11.62 (1H, s, N–H), 7.98 (1H, s, N=C–H), 4.81 (2H, s, –CH_2), (*trans*, 18%) 11.71 (s, N–H), 8.18 (s, N=C–H), 4.41 (s, –CH_2), (*cis* + *trans*) 4.27–4.39 (∼5H, m, CH_2-spiro), 5.16 (3H, s, CH_2–O) 6.98–7.89 (∼17H, m, Ar–H); ^{13}C NMR (75 MHz, DMSO-d_6) δ; (*cis*, 82%) 173.3, 167.8, 147.5, 41.1, (*trans*, 18%) 173.1, 163.0, 144.5, 41.5, (*cis* + *trans*) 66.0, 69.8, 101.9, 110.2, 115.6, 123.3, 123.5, 124.2, 124.9, 127.2, 128.2, 128.4, 128.9, 129.0, 129.2, 132.0, 137.2, 144.3, 144.4, 160.3, 160.4; LC-MS (negative mode) $[M–H]^-$ = 456.0 *m*/*z*.

2.3.2. *N*′-(4-Nitrobenzylidene)-2-(2-oxospiro[indoline-3,2′-[1,3]dioxolan]-1-yl)acetohydr azide (2). Light yellow crystals; yield 80%; m.p. 266–267 °C; FT-IR $\bar{\upsilon}$ (cm^{-1}); 33 154 (N–H), 3089 (C_{sp^2}–H), 1731 (C=O, spiroisatin), 1694 (C=O, acetohydrazide), 1618 (C=N imine str.), 1265 (C–N, lactam), 1135 (C–O–C), 1515, 1341 (N–O); ^{1}H NMR (300 MHz, DMSO-d_6) δ; (*cis*, 76%) 12.07 (1H, B, N–H), 8.14 (1H, s, N=C–H), 4.90 (2H, s, CH_2), (*trans*, 24%) 12.07 (1H, B, N–H), 8.34 (1H, s, N=C–H), 4.47 (s, CH_2), (*cis* + *trans*) 4.28–4.39 (∼6H, m, CH_2-spiro), 7.02–8.31 (∼11H, m, Ar–H); ^{13}C NMR (75 MHz, DMSO-d_6) δ; (*cis*, 76%) 173.3, 168.5, 148.2, 41.2, (*trans*, 24%) 173.2, 163.8, 144.4, 41.9, (*cis* + *trans*) 66.0, 101.9, 110.3, 123.4, 124.2, 128.4, 132.0, 140.6, 142.2, 144.2; LC-MS (negative mode) $[M–H]^-$ = 395.1 *m*/*z*.

2.3.3. *N*′-(2-Hydroxybenzylidene)-2-(2-oxospiro[indoline-3,2′-[1,3]dioxolan]-1-yl)acetoh ydrazide (3). White crystals; yield 74%; m.p. 249–250 °C; FT-IR $\bar{\upsilon}$ (cm^{-1}); 3161 (N–H), 3065 (C_{sp^2}–H), 1743 (C=O, spiroisatin), 1677 (C=O, acetohydrazide), 1687 (C=N imine str.), 1264 (C–N, lactam), 1137 (C–O–C); ^{1}H NMR (300 MHz, DMSO-d_6) δ: (*cis*, 60%) 11.67 (s, N–H), 10.06 (s, O–H) 8.35 (s, N=C–H), 4.82 (s, CH_2), (*trans*, 40%) 12.05 (1H, s, N–H), 10.94 (1H, s, O–H), 8.45 (1H, s, N=C–H), 4.45 (1H, s, CH_2) (*cis* + *trans*) 4.27–4.41 (∼6H, m, CH_2-spiro), 6.84–7.78 (∼13H, m, Ar–H); ^{13}C NMR (75 MHz, DMSO-d_6) δ; (*cis*, 60%) 173.3, 167.7, 147.8, 41.4, (*trans*, 40%) 173.2, 163.1, 144.5, 41.0, (*cis* + *trans*) 66.0, 101.9, 110.2, 110.3, 116.5, 116.8, 119.0, 119.8, 120.5, 123.3, 123.5, 124.2, 124.9, 125.0, 126.7, 129.5, 132.0, 141.9, 144.2; LC-MS (negative mode) $[M–H]^-$ = 366.0 *m*/*z*.

2.4. Quantum-based studies

Non-Covalent Interaction (NCI) analyses were done with Multiwfn[47] software. For the NCI plots, we used VMD[48] graphical visualization software. Guassian09 suite quantum chemistry program[49] was used to optimize the geometry of *N*-acyl hydrazones. We utilized this basis sets B3LYP/6-311++G (d,p)[50] and optimized the structure of our acylhydrazones in DMSO (solution) form to compare the conformations and calculated the difference in their energies. To evaluate the potential energy surface (PES) graph, the Guassian09 suite quantum chemistry program was used with basis sets B3LYP/6-311++G (d,p) on the dihedral angle O28–C23–N27–N29.

3. Results and discussion

Spiroisatin-based *N*-acyl hydrazones **1–3** (Fig. 2) were synthesized in four steps, starting from the inexpensive and readily available isatin (Scheme S1, ESI†). First, the 3-carbonyl group of isatin was protected, followed by a reaction with ethyl bromoacetate in the second step. The resulting intermediate (**I**) was then treated with hydrazine hydrate to form the corresponding hydrazides (**II**), which were subsequently reacted with three different aldehydes to produce the target spiroisatin-based *N*-acyl hydrazones **1–3**. Isatin was selected due to its biological relevance and its ability to enhance the electrophilicity of the adjacent CH_2 group through nitrogen lone pair delocalization, making it more prone to non-covalent C-bonding interactions. Three aldehydes were chosen based on their electronic characteristics: one with a benzyloxy electron-donating group at the *para* position, another with a strong electron-withdrawing nitro group, both of which modulate the electron density at the imine nitrogen and influence its involvement in C-bonding. The third aldehyde, featuring an *ortho*-hydroxy group, was selected to investigate the competition between intramolecular C-bonding and intramolecular hydrogen bonding with imine nitrogen (Fig. 2).

Interestingly, the solution-state NMR studies of compound **1** in DMSO-d_6 reveal the isomerization of the amide bond, resulting in a rotameric mixture of *cis* and *trans* isomers, with the *cis* conformation being dominant, accounting for 82% of the mixture (Fig. 3). The predominance of the *cis* isomer can be attributed to intramolecular C-bonding interactions involving the lone pair of the imine nitrogen [$N_{(lp)}$] and the $\sigma^*_{CH_2}$ orbital, which stabilizes the *cis* form. Without this stabilization, steric factors would favor the *trans* isomer.[34–37] Similarly, compounds **2** and **3** also exhibit a *cis*-dominated rotameric mixture, with 76% and 60%, respectively of the *cis* isomer (Fig. S1 & S2†). The lower percentage of *cis* conformation of **3** as compared to the

 © 2025 The Author(s). Published by the Royal Society of Chemistry

Open Access Article. Published on 13 January 2025. Downloaded on 2/14/2026 10:03:16 PM.
This article is licensed under a Creative Commons Attribution-NonCommercial 3.0 Unported Licence.

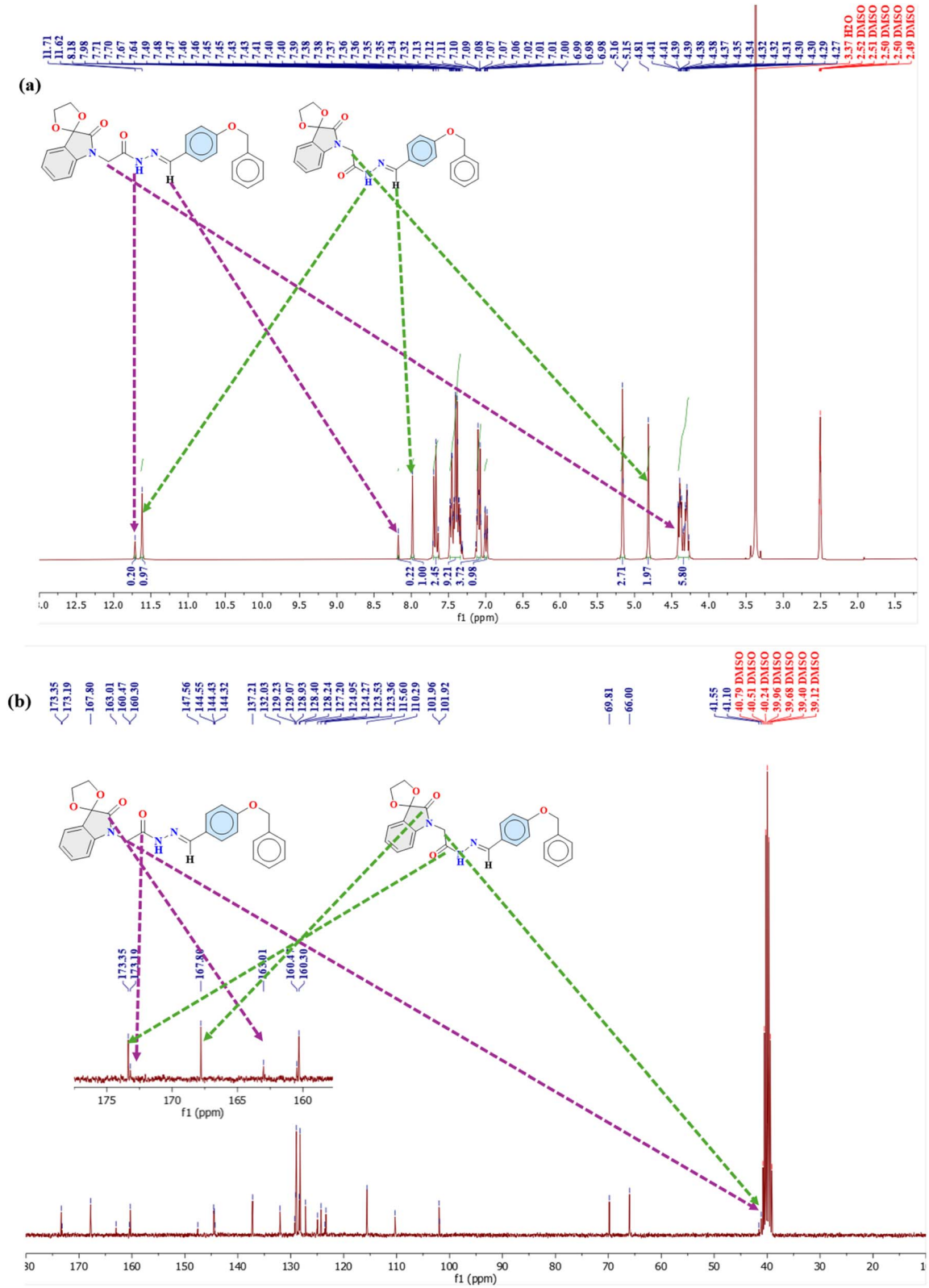

Fig. 3 The representative spectra of compound **1**; (a) ^{1}H NMR, (b) ^{13}C NMR.

compounds **1** and **2** can tentatively attributed to the competing intramolecular H-bonding that exists between the *o*-hydroxy group and the imine nitrogen, resulting in the relatively lower percentage of *cis* isomer. The higher percentage of the *cis* isomer of compound **1** (82%) than the *cis* isomer of compound **2** (76%) however is credited to electronic factors owing to the

Open Access Article. Published on 13 January 2025. Downloaded on 2/14/2026 10:03:16 PM.
This article is licensed under a Creative Commons Attribution-NonCommercial 3.0 Unported Licence.

Table 1 ^{1}H NMR chemical shifts of compounds **1–3**

	Chemical shift δ (ppm)						
	C(O)–NH		N=C–H		CH_2–C(O)		Percentage isomeric ratio
Compounds	*Trans*	*Cis*	*Trans*	*Cis*	*Trans*	*Cis*	*Cis* : *Trans*
1	11.71	11.62	8.18	7.98	4.41	4.81	82 : 18
2	12.07[a]	12.07[a]	8.34	8.14	4.47	4.90	76 : 24
3	12.05	11.67	8.45	8.35	4.45	4.82	60 : 40

[a] Broad.

Table 2 Chemical shifts of compounds **1–3** in ^{13}C NMR spectra

	Chemical shift δ (ppm)							
	CH_2–^{13}C(O)–NH		^{13}C(O)–N (spiroisatins)		N=^{13}C–H		$^{13}CH_2$–C(O)	
Compounds	*Trans*	*Cis*	*Trans*	*Cis*	*Trans*	*Cis*	*Trans*	*Cis*
1	173.1	173.3	163.0	167.8	144.5	147.5	41.5	41.1
2	173.2	173.3	163.8	168.5	144.4	148.2	41.9	41.2
3	173.2	173.3	163.1	166.7	144.5	147.8	41.4	41.0

presence of two different substituents at the *para* position of the aryl ring. The electron-donating group like the benzyloxy group present at the *para* position of the aryl ring of compound **1**, makes the imine moiety more electron-rich, and thus a strong C-bond acceptor. On the other hand, the electron-withdrawing *nitro* group in compound **2** likely withdraws the electron density from the imine moiety, making it relatively less susceptible to make intramolecular C-bond. Notably, the equilibrium showing 40% of the *trans* isomer for compound **3** on the NMR timescale suggests a low energy barrier between the *cis* and *trans* conformers, allowing for rapid interconversion. This low energy barrier and the possibility of rapid conformational exchange are further supported by quantum-based studies (*vide infra*).

The presence of both isomers in the solution is evident from the distinct proton signals observed in their NMR spectra (Fig. 3a, S1a and S2a†). Generally, the protons of the *trans* isomer are more deshielded (downfield) compared to those of the *cis* isomer.[40,51] For instance, in compound **1**, the NH proton resonates at 11.62 ppm for the *cis* isomer, while for the *trans* isomer, it appears downfield at 11.71 ppm (Fig. 3a, Table 1). Similarly, the N=C–H proton resonates at 7.98 ppm for the *cis* isomer and at 8.18 ppm for the *trans* isomer. The CH_2 protons play a crucial role in distinguishing between the *cis* and *trans* conformations, as the attached carbon serves as the C-bond donor. In the *cis* isomer, the lone pair on the imine nitrogen interacts with the $\sigma^*_{CH_2}$ orbital of the CH_2 group, leading to a slight elongation of the C–H bond within the methylene group. This interaction results in greater deshielding of the methylene protons, causing a downfield shift in the *cis* conformation. In contrast, this interaction is absent in the *trans* isomer, resulting in an upfield shift of these protons. Specifically, in the *cis* isomer, the methylene protons resonate as a singlet at 4.81 ppm, whereas in the *trans* conformer, their resonance slightly overlaps with the multiplets of the diastereotopic protons at the 3-position of the isatin ring, appearing at 4.41 ppm (Fig. 3a, Table 1).

Likewise, the ^{13}C NMR spectra of compounds **1–3** exhibit two distinct sets of signals corresponding to the *cis* and *trans* isomers (Fig. 3b, S1b, S2b† and Table 2). For example, the methylene carbon in compound **1**, which participates in C-bonding, resonates at 41.5 ppm for the *trans* isomer, and a slightly more shielded signal at 41.1 ppm for the *cis* isomer appeared, indicating intramolecular interactions that shield the methylene group in the *cis* form through $N_{(lp)} \rightarrow \sigma^*_{CH_2}$ interactions.[40,51] Due to the cyclic nature of isatin, the amide carbonyl of the cyclic amide typically appears more shielded (upfield) than that of the acyclic hydrazone amide. This is evident in the observed carbonyl signals: the amide carbonyl of the hydrazone resonates at 173.1 ppm for the *trans* isomer and 173.3 ppm for the *cis* isomer, whereas the cyclic isatin amide appears at 163.0 ppm for the *trans* isomer and 167.8 ppm for the *cis* isomer (Fig. 3b, Table 2).

As anticipated and consistent with the solution-state results, the solid-state structures (Table S1†) of spiroisatin-based *N*-acyl hydrazones **1** and **2** are confirmed to adopt a *cis* conformation (Fig. 4a and b). This preference arises from the alignment of the lone pair on the sp^2-hybridized nitrogen atom with the antibonding $\sigma^*_{CH_2}$ orbital of the $CH_{2(sp^3)}$–N bond, resulting in the formation of non-covalent C-bonding interactions (N⋯C distance 2.740 Å for **1** and 2.707 Å for **2**). In contrast, the solid-state structure of compound **3** is found to adopt a *trans*

© 2025 The Author(s). Published by the Royal Society of Chemistry

Open Access Article. Published on 13 January 2025. Downloaded on 2/14/2026 10:03:16 PM.
This article is licensed under a Creative Commons Attribution-NonCommercial 3.0 Unported Licence.

conformation (Fig. 4c), most probably due to a dominant intramolecular hydrogen bond [O(2)–H(1B)···N(2) 1.822 Å] between the imine nitrogen and the hydroxyl group located at the *ortho* position of the adjacent aromatic ring, and additionally due to packing factors (Fig. S2†). Two previous searches[39] in the Cambridge Structural Database (CSD) also support these findings. In search A (Fig. S3†), where both *ortho* positions of the aromatic ring were unsubstituted, the *cis* conformation was predominant in 16 out of 20 structures, likely due to the stabilization provided by non-covalent N···C, C-bonding interactions. In contrast, in search B (Fig. S3†), where at least one *ortho* position was substituted by a hydroxyl group, the *trans* conformation was more common. This *trans* preference can be collectively attributed to the strong intramolecular O–H···N hydrogen bond, steric influence, and the solid state packing effects. The representative structure from search A, TIGNED, exhibits the *cis* conformation and shows clear evidence of C–bonding interaction (N···C distance 2.73 Å) (Fig. S4†). On the other hand, the representative structure EYEKOK from search A, with a *trans* amide conformation, suggests that other strong non-covalent interactions in the crystal packing (Fig. S4†) stabilize the less favored *trans* conformation. The predominance of the *cis* conformation in search A underscores the importance of σ-hole interactions in promoting the *cis* isomer. In search B, the representative *trans* conformation structure AYAFAH exhibits a strong intramolecular hydrogen bond that blocks the lone pair on the nitrogen atom, preventing C-bonding. However, in the representative structure YUPSEJ (N···C distance 2.75 Å), despite the presence of an *ortho* OH group, the *cis* conformation is observed. This is because, in two

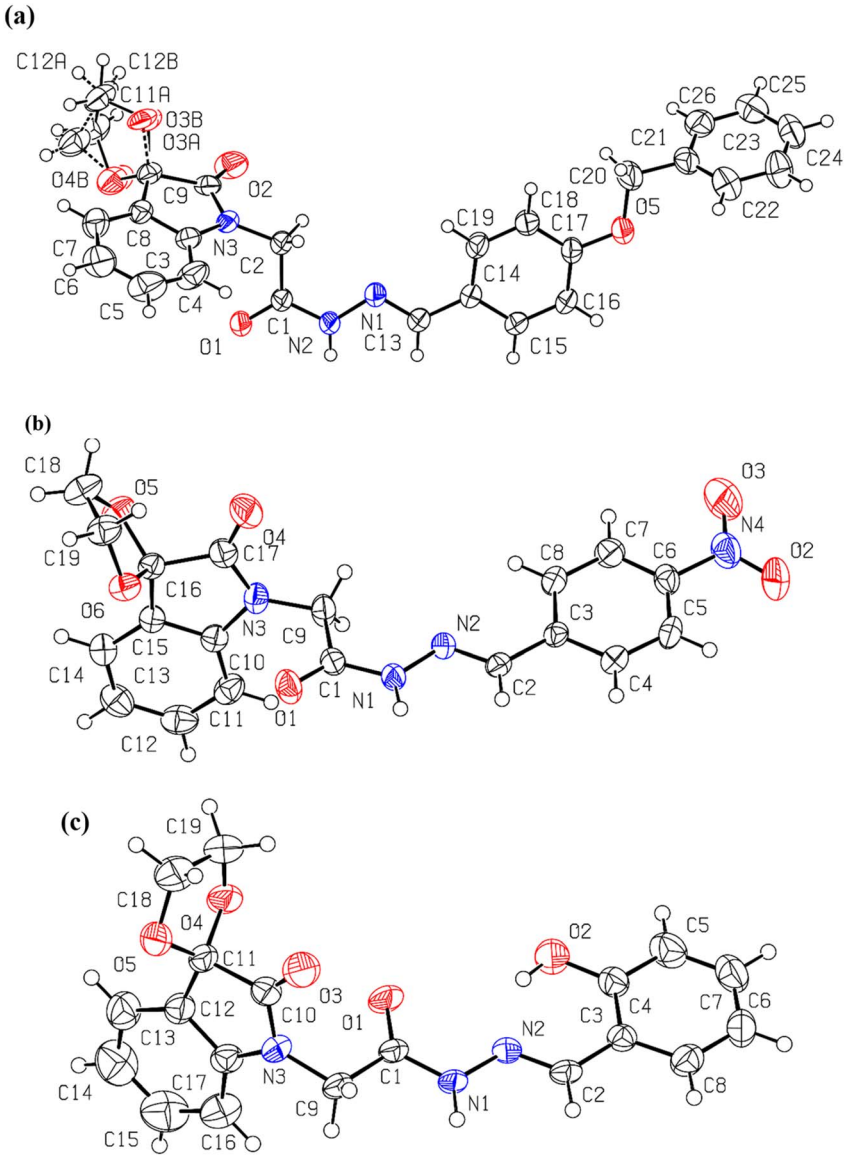

Fig. 4 The molecular structure of compounds (a) **1** [C(2)···N(1) 2.740 Å, N(3)–C(2)···N(1) 171.89°]; (b) **2** [C(9)···N(2) 2.707 Å, N(3)–C(9)···N(2) 169.31°]; (c) **3**. Displacement ellipsoids drawn at the 50% probability level.

Open Access Article. Published on 13 January 2025. Downloaded on 2/14/2026 10:03:16 PM.
This article is licensed under a Creative Commons Attribution-NonCommercial 3.0 Unported Licence.

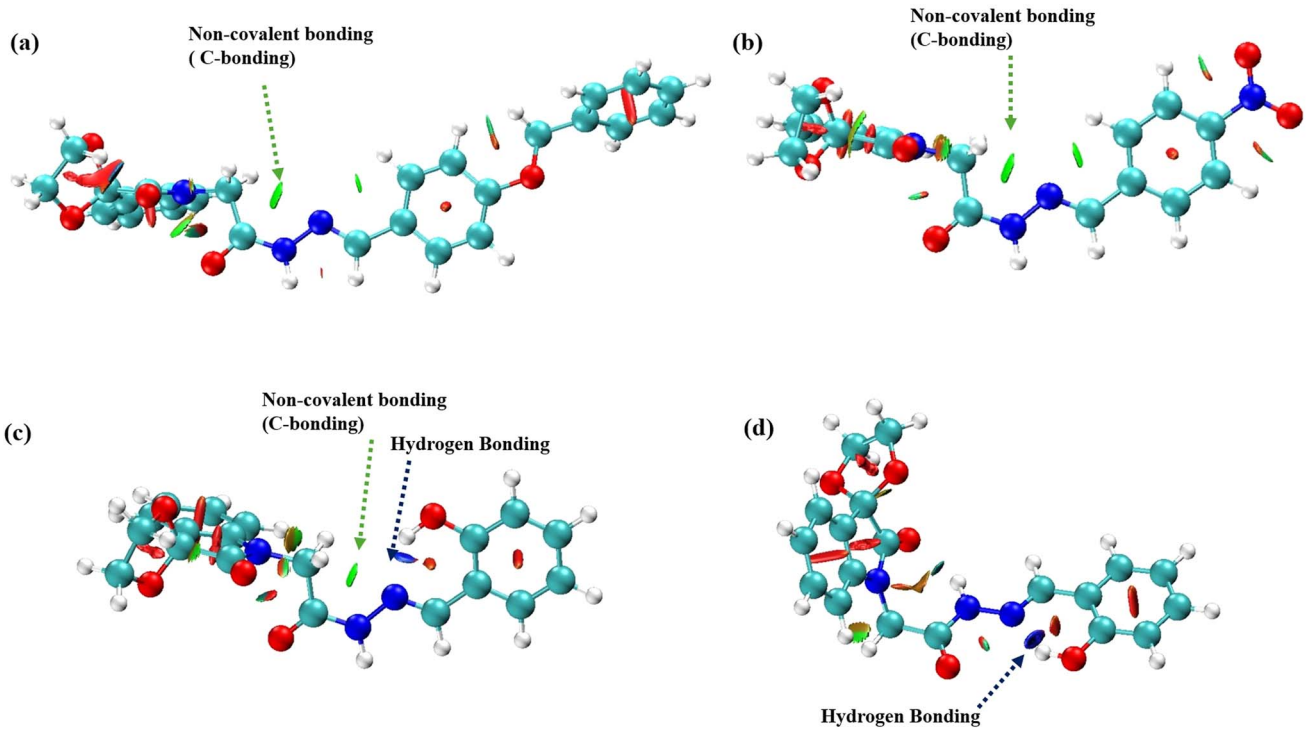

Fig. 5 NCI plots of spiroisatin-based *N*-acyl hydrazones **1–3** showing, (a) C-bonding in **1**, (b) C-bonding in **2**, C-bonding in **2**, (c) C-bonding and H-bonding in **3**, (d) intramolecular H-bonding in **3**.

out of four cases found in the literature, the OH group forms an intramolecular hydrogen bond with a *meta*-positioned group on the same ring, freeing the nitrogen's lone pair to interact with the carbon atom, thus favoring the *cis* conformation (Fig. S4†). Additionally, the formation of a stable amide–amide dimer synthon in the solid state further stabilizes the *cis* arrangement in this case.[39]

The $N_{(lp)} \rightarrow \sigma^*_{CH_2}$ interactions in compounds **1–3** were visualized using the mutliwfn[47] to generate non-covalent interaction (NCI) plots.[52] NCI plots are advanced visualization tools that go beyond identifying critical points, offering a detailed representation of non-covalent interactions through isosurfaces. These plots are based on electron density and utilize the sign of the second Hessian eigenvalues and color coding to distinguish between favorable and unfavorable interactions. However, the information provided by NCI plots is primarily qualitative, highlighting regions that may be prone to interaction. The color codes represent different types of interactions: red indicates repulsive interactions, blue signals strong attractive interactions, green represents weaker interactions such as C-bonding, and yellow denotes weaker repulsive forces. The NCI plots for spiroisatin-based *N*-acyl hydrazones **1–3**, in solution phase are shown in Fig. 5. The sp^2 nitrogen atom participates in C-bonding interactions involving the σ-hole of the CH_2 group, as well as weak hydrogen bonding with the *ortho* hydrogen of the phenyl ring, observed in the *cis* isomers of compounds **1** and **2** (Fig. 5a and b). In compound **3**, strong hydrogen bonding is observed, indicated by the blue color in the NCI plot. In the *cis* conformer of **3**, both C-bonding and hydrogen bonding are present (Fig. 5c), while in the *trans* conformer, only hydrogen bonding is observed (Fig. 5d).

The geometry optimization and energy calculations were calculated with natural bond orbital (NBO) analysis utilizing the basis sets B3LYP/6-311++G (d,p)[50] at full NBO level. NBO[53,54] analysis of representative spiroisatin-based *N*-acyl hydrazone **2** revealed the existence of $N_{(lp)} \rightarrow \sigma^*_{CH_2}$ noncovalent interactions between the lone pair of the imine nitrogen and the σ-hole of the CH_2 group (Fig. 6). Furthermore, it was determined that the methylene group acts as a C-bond donor, while the nitrogen with a free lone pair serves as the C-bond acceptor.

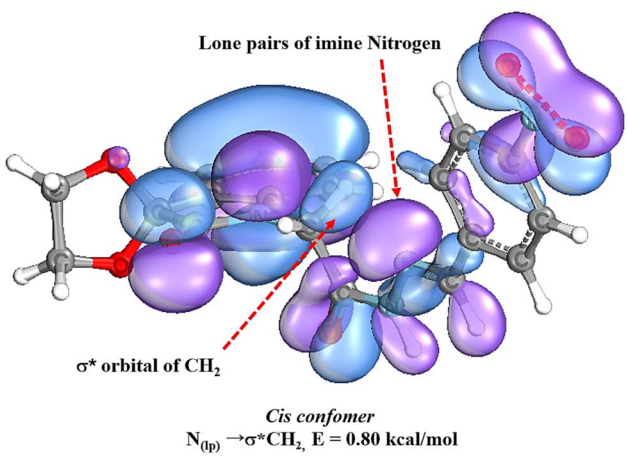

Fig. 6 NBO analysis showing $N_{(lp)} \rightarrow \sigma^*_{CH_2}$ interactions in *cis* isomer of **2**.

© 2025 The Author(s). Published by the Royal Society of Chemistry

Open Access Article. Published on 13 January 2025. Downloaded on 2/14/2026 10:03:16 PM.
This article is licensed under a Creative Commons Attribution-NonCommercial 3.0 Unported Licence.

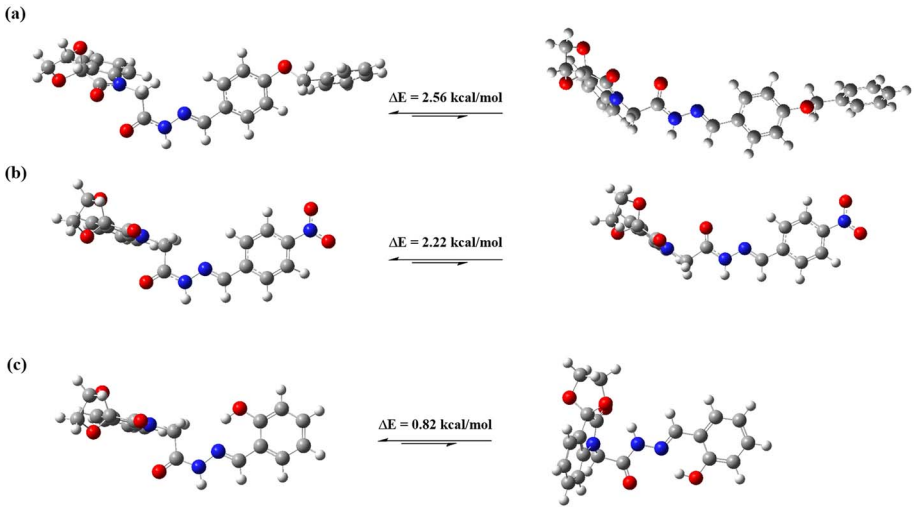

Fig. 7 Optimized structures and calculated energy barriers between *cis* and *trans* isomers of compounds, (a) **1**, (b) **2**, (c) **3**.

Table 3 The energies for compounds **1–3** in DMSO

	Energies (Hartree) (*trans*)	Energies (Hartree) (*cis*)	Δ*E* (Hartree) (*cis–trans*)	Δ*E* (kcal mol^{-1}) (*cis–trans*)
1	−1527.039505	−1527.043588	−0.004083	−2.56
2	−1387.840919	−1387.844468	−0.003549	−2.22
3	−1260.000433	−1260.001748	−0.001315	−0.82

Finally, the quantum chemical calculations[55] were performed to validate our solution-state results. The structures of compounds **1–3** were optimized in DMSO to compare their conformations, and the energy differences were calculated using the B3LYP/6-311++G(d,p)[50] basis set. The optimized geometries indicated that the structure of the spiroisatin-based *N*-acylhydrazones is not planar. However, the acyl hydrazone functional group and the phenyl ring of the hydrazone exhibit planarity relative to each other (Fig. 7). For compounds **1** and **2**, the *trans* isomers have higher energies, while the *cis* isomers exhibit lower energies in DMSO (Table 3). Specifically, for compound **1**, the energy difference between the *cis* and *trans* isomers is −2.56 kcal mol^{-1}, while for compound **2**, the energy barrier is −2.22 kcal mol^{-1}. The subtle energy difference between compounds **1** and **2** suggests that the *cis* conformer of **1** is slightly more stable than that of **2**, likely due to the electron-donating effect of the benzyloxy group. These results also indicate that the *cis* isomer remains stable even in highly polar solvents with high relative permittivity, as the $N_{(lp)} \rightarrow \sigma^*_{CH_2}$ C–bonding interaction can persist in solution. In the case of compound **3**, the energy barrier between the *cis* and *trans* isomers is reduced to a minimal value of −0.82 kcal mol^{-1}, as both isomers are stabilized by stronger intermolecular hydrogen bonding between the *o*-hydroxy group and the imine nitrogen atom. Due to this small energy difference, the *cis* and *trans* forms of **3** can rapidly interconvert, resulting in a higher proportion of the *trans* form (40%) observed in the NMR studies compared to the *trans* isomers of compounds **1** (18%) and **2** (24%) (*vide supra*).

The conformational and rotational equilibria exhibit significant variation depending on the medium.[56,57] It is important to note that the Gibbs free energy differences between conformational or rotational isomers are very small, and the solvation enthalpies must be considerably larger than these free energies in order to induce a substantial shift in the equilibrium position. While highly polar solvents like DMSO can diminish intermolecular interactions, the predominance of *cis* isomers of compounds **1–3** in solution, driven by intramolecular C-bonding interactions involving $N_{(lp)} \rightarrow \sigma^*_{CH_2}$ clearly indicate the high polarity of the *cis* isomer *i.e.*, the isomer with greater dipole moment is more stable in polar solvents like DMSO.[56,58,59] Therefore, these quantum-based results are in good agreement with the findings of our solution-phase studies.

To determine the stable conformation in DMSO, conformational analysis was performed by sampling points on potential energy. A relaxed potential energy scan was done on the dihedral angle O28–C23–N27–N29 *i.e.*, a standard rotatable bond. The scan was performed from −180° to 180° with every 20° increment. Compound **1** served as a model for these studies. The minimum energy conformation can be found when the θ (dihedral angle) = −0.94°, −179.48°, and 179.48°. Two same conformations, *i.e.*, *cis* conformer is present when $\theta = -179.48°$, and 179.48°. Likewise, when $\theta = -0.94°$, *trans* was observed. A minute difference of −0.004083 Hartree (−2.56 kcal mol^{-1}) is found between these two conformers. This subtle energy difference confirms that these two conformers can easily coexist in solution form without any large energy barrier. Moreover, the

Open Access Article. Published on 13 January 2025. Downloaded on 2/14/2026 10:03:16 PM.
This article is licensed under a Creative Commons Attribution-NonCommercial 3.0 Unported Licence.

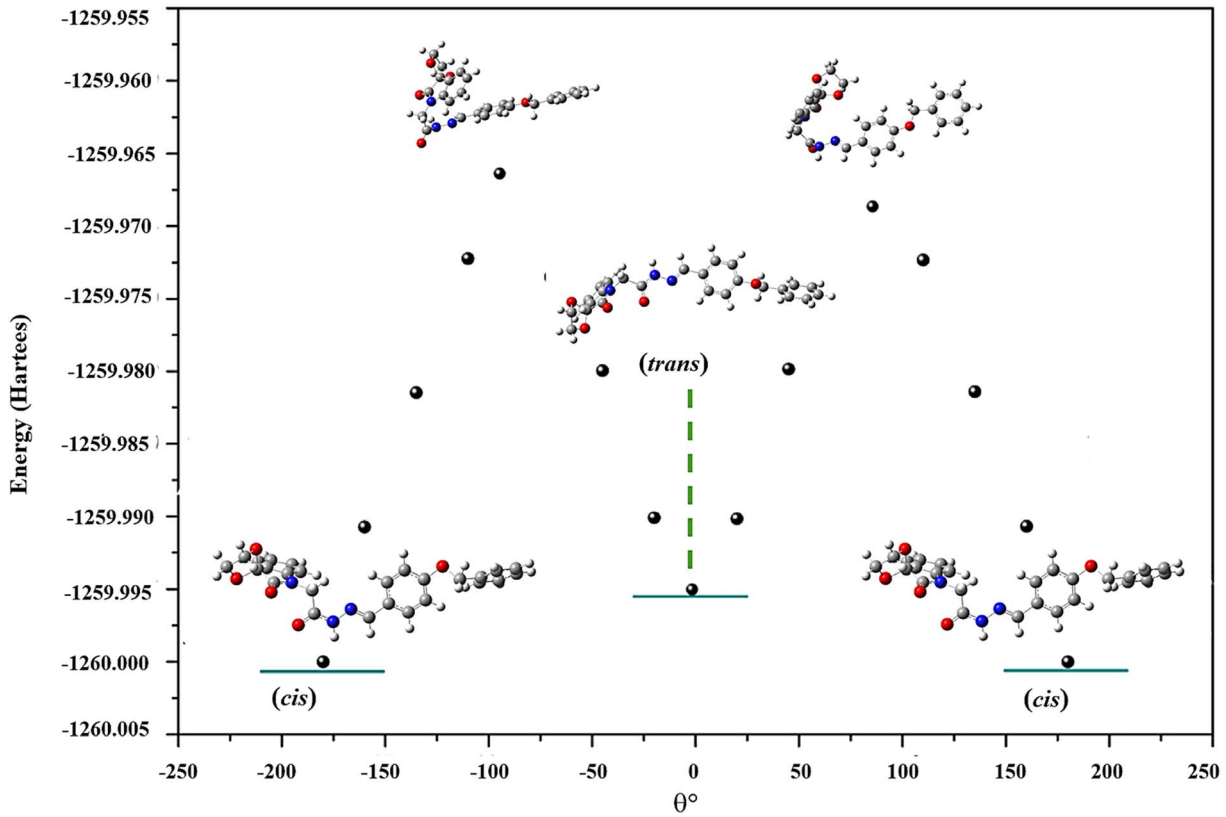

Fig. 8 PES-scan of compound **1** with dihedral angle O28–C23–N27–N29.

maxima at the graph indicated the transition geometries between *cis* and *trans*-conformers at $\theta = -0.049°$ (energy = −1527.04187 Hartree), and 0.107° (energy = −1527.04338 Hartree) (Fig. 8). These sorts of potential energy surface (PES) scans were also undergone for **2** and **3** (Fig. S6 and S7†).

4. Conclusion

In conclusion, we have highlighted the importance of intramolecular C-bonding in stabilizing a particular conformation in spiroisatin-based *N*-acyl hydrazones **1–3**. Despite the steric preference for a *trans* geometry around the NH–amide bond, C-bonding ($N_{(lp)} \rightarrow \sigma^*_{CH_2}$ interactions) significantly stabilizes the *cis* isomer of compounds **1** and **2**, as evidenced by ^{1}H and ^{13}C NMR, X-ray diffraction, and density functional theory (DFT) calculations. In DMSO-d_6, compounds **1** and **2** predominantly adopt the *cis* form (82% and 76%, respectively), while compound **3** shows a slightly reduced *cis* preference (60%) due to competing hydrogen bonding. Single-crystal X-ray studies confirmed *cis* predominance for compounds **1** and **2**, with compound **3** crystallizing in the *trans* form, likely due to packing and hydrogen bonding effects. Minimal energy barriers between *cis* and *trans* forms, supported by DFT calculations and potential energy surface scans, suggest dynamic equilibrium in polar solvents. The stabilization of *cis* conformation even in a highly polar solvent clearly indicates the broader significance of this interaction in supramolecular chemistry, especially when it is intramolecularly present.

Data availability

The crystallographic data for **1–3** and other data related to this article is available in the ESI.†

Author contributions

Muhammad Imran Ali investigation, methodology, formal analysis, writing – original draft writing, Javid Hussain formal analysis, visualization Muhammad Usman Anwar data curation, software, Ahmed Al-Harrasi resources, formal analysis, Muhammad Moazzam Naseer conceptualization, funding acquisition, resources, project administration, writing – review & editing.

Conflicts of interest

There are no conflicts to declare.

Acknowledgements

MMN is grateful to The World Academy of Sciences (TWAS) for financial support through Project No. 13-419 RG/PHA/AS_CUNESCO FR: 3240279216.

© 2025 The Author(s). Published by the Royal Society of Chemistry

Open Access Article. Published on 13 January 2025. Downloaded on 2/14/2026 10:03:16 PM. This article is licensed under a Creative Commons Attribution-NonCommercial 3.0 Unported Licence.

References

1 A. S. Mahadevi and G. N. Sastry, Cooperativity in noncovalent interactions, *Chem. Rev.*, 2016, **116**, 2775–2825, DOI: 10.1021/cr500344ed.

2 M. Dubecky, L. Mitas and P. Jurecka, Noncovalent interactions by quantum Monte Carlo, *Chem. Rev.*, 2016, **116**, 5188–5215, DOI: 10.1021/acs.chemrev.5b00577.

3 D. Chatterji, *Basics of Molecular Recognition*, CRC Press, Boca Raton, 1st edn, 2016, DOI: 10.1201/b19645.

4 F. Weinhold and R. A. Klein, What is a hydrogen bond? Mutually consistent theoretical and experimental criteria for characterizing H-bonding interactions, *Mol. Phys.*, 2012, **110**, 565–579, DOI: 10.1080/00268976.2012.661478.

5 A. Mukherjee, S. Tothadi and G. R. Desiraju, Halogen bonds in crystal engineering: like hydrogen bonds yet different, *Acc. Chem. Res.*, 2014, **47**, 2514–2524, DOI: 10.1021/ar5001555.

6 B. K. Saha, A. Nangia and M. Jaskólski, Crystal engineering with hydrogen bonds and halogen bonds, *CrystEngComm*, 2005, **7**, 355–358, DOI: 10.1039/b501693b.

7 D. W. Zhang, J. Tian, L. Chen, L. Zhang and Z. T. Li, Dimerization of Conjugated Radical Cations: An Emerging Non-Covalent Interaction for Self-Assembly, *Chem.–Asian J.*, 2015, **10**, 56–68, DOI: 10.1002/asia.201402805.

8 C. B. Aakeröy, Crystal engineering: strategies and architectures, *Acta Crystallogr., Sect. B: Struct. Sci.*, 1997, **53**, 569–586, DOI: 10.1107/s0108768197008446.

9 A. S. Novikov, *Non-covalent interactions in coordination and organometallic chemistry*, 2020, DOI: 10.3390/books978-3-0365-3287-5.

10 Z. Berkovitch-Yellin and L. Leiserowitz, The role played by C–H···O and C–H···N interactions in determining molecular packing and conformation, *Acta Crystallogr., Sect. B: Struct. Sci.*, 1984, **40**, 159–165, DOI: 10.1107/s0108768184001919.

11 Y. Gu, T. Kar and S. Scheiner, Fundamental properties of the CH···O interaction: is it a true hydrogen bond?, *J. Am. Chem. Soc.*, 1999, **121**, 9411–9422, DOI: 10.1021/ja991795g.

12 M. Brandl, M. S. Weiss, A. Jabs, J. Sühnel and R. Hilgenfeld, CH···π-interactions in proteins, *J. Mol. Biol.*, 2001, **307**, 357–377, DOI: 10.1006/jmbi.2000.4473.

13 Z. Zhang, Y. Luo, J. Chen, S. Dong, Y. Yu, Z. Ma and F. Huang, Formation of Linear Supramolecular Polymers That Is Driven by C-H···π Interactions in Solution and in the Solid State, *Angew. Chem., Int. Ed.*, 2011, **50**, 1397, DOI: 10.1002/ange.201006693.

14 R. Parthasarathi, V. Subramanian and N. Sathyamurthy, Hydrogen bonding without borders: an atoms-in-molecules perspective, *J. Phys. Chem. A*, 2006, **110**, 3349–3351, DOI: 10.1021/jp060571z.

15 S. Scheiner, T. Kar and Y. Gu, Strength of the CαH···O hydrogen bond of amino acid residues, *J. Biol. Chem.*, 2001, **276**, 9832–9837, DOI: 10.1074/jbc.M010770200.

16 M. Nishio, M. Hirota and Y. Umezawa, *The CH/π Interaction: Evidence, Nature, and Consequences*, John Wiley & Sons, 1st edn, 1998.

17 M. J. Plevin, D. L. Bryce and J. Boisbouvier, Direct Detection of CH/π Interactions in Proteins, *Nat. Chem.*, 2010, **2**, 466–471, DOI: 10.1038/nchem.650.

18 C. A. Sacksteder, S. L. Bender and B. A. Barry, Role for Bound Water and CH–π Aromatic Interactions in Photosynthetic Electron Transfer, *J. Am. Chem. Soc.*, 2005, **127**, 7879–7890, DOI: 10.1021/ja050659a.

19 J. Y. Lim, I. Marques, A. L. Thompson, K. E. Christensen, V. Félix and P. D. Beer, Chalcogen bonding macrocycles and [2] rotaxanes for anion recognition, *J. Am. Chem. Soc.*, 2017, **139**, 3122–3133, DOI: 10.1021/jacs.6b12745.

20 G. E. Garrett, E. I. Carrera, D. S. Seferos and M. S. Taylor, Anion recognition by a bidentate chalcogen bond donor, *Chem. Commun.*, 2016, **52**, 9881–9884, DOI: 10.1039/c6cc04818h.

21 A. Bauzá and A. Frontera, Chalcogen 'like-like' interactions involving trisulphide and triselenide compounds: a combined CSD and *ab initio* study, *Molecules*, 2018, **23**, 699, DOI: 10.3390/molecules23030699.

22 M. D. Esrafili and A. Sadr-Mousavi, Modulating of the pnicogen-bonding by a H···π interaction: an *ab initio* study, *J. Mol. Graphics Modell.*, 2017, **75**, 165–173, DOI: 10.1016/j.jmgm.2017.04.017.

23 R. Lo, P. Švec, Z. Růžičková, A. Růžička and P. Hobza, On the nature of the stabilisation of the E···π pnicogen bond in the $SbCl_3$···toluene complex, *Chem. Commun.*, 2016, **52**, 3500–3503, DOI: 10.1039/c5cc10363k.

24 Y. V. Nelyubina, A. A. Korlyukov and K. A. Lyssenko, Experimental charge density evidence for pnicogen bonding in a crystal of ammonium chloride, *ChemPhysChem*, 2015, **16**, 676–681, DOI: 10.1002/cphc.201402673.

25 M. D. Esrafili and A. Sabouri, Carbene–aerogen bonds: an *ab initio* study, *Mol. Phys.*, 2017, **115**, 971–980, DOI: 10.1080/00268976.2017.1297864.

26 M. D. Esrafili and F. Mohammadian-Sabet, An *ab initio* study on anionic aerogen bonds, *Chem. Phys. Lett.*, 2017, **667**, 337–344, DOI: 10.1016/j.cplett.2016.11.019.

27 A. Bauzá, T. J. Mooibroek and A. Frontera, Small Cycloalkane $(CN)_2C\text{-}C(CN)_2$ Structures Are Highly Directional Non-covalent Carbon-Bond Donors, *Chem.–Eur. J.*, 2014, **20**, 10245–10248, DOI: 10.1002/chem.201403680.

28 A. Bauzá, T. J. Mooibroek and A. Frontera, Non-covalent sp^3 carbon bonding with $ArCF_3$ is analogous to CH–π interactions, *Chem. Commun.*, 2014, **50**, 12626–12629, DOI: 10.1039/c4cc05602g.

29 X. García-LLinás, A. Bauzá, S. K. Seth and A. Frontera, Importance of R–CF_3···O tetrel bonding interactions in biological systems, *J. Phys. Chem. A*, 2017, **121**, 5371–5376, DOI: 10.1021/acs.jpca.7b06052.

30 P. Politzer, J. S. Murray and T. Clark, in *Halogen bonding I: Impact on Materials Chemistry and Life Sciences*, Springer, Cham, 2015, pp. 19–42, doi: DOI: 10.1007/128_2014_568.

31 P. Politzer, J. S. Murray, T. Clark and G. Resnati, The σ-hole revisited, *Phys. Chem. Chem. Phys.*, 2017, **19**, 32166–32178, DOI: 10.1039/c7cp06793c.

© 2025 The Author(s). Published by the Royal Society of Chemistry

Open Access Article. Published on 13 January 2025. Downloaded on 2/14/2026 10:03:16 PM. This article is licensed under a Creative Commons Attribution-NonCommercial 3.0 Unported Licence.

32 D. Mani and E. Arunan, The X–C···Y (X = O/F, Y = O/S/F/Cl/Br/N/P) 'carbon bond' and hydrophobic interactions, *Phys. Chem. Chem. Phys.*, 2013, **15**, 14377–14383, DOI: 10.1039/c3cp51658j.

33 S. P. Thomas, M. S. Pavan and T. G. Row, Experimental evidence for 'carbon bonding' in the solid state from charge density analysis, *Chem. Commun.*, 2014, **50**, 49–51, DOI: 10.1039/c3cc47226d.

34 A. Jabs, M. S. Weiss and R. Hilgenfeld, Non-proline *cis* peptide bonds in proteins, *J. Mol. Biol.*, 1999, **286**, 291–304, DOI: 10.1006/jmbi.1998.2459.

35 D. E. Stewart, A. Sarkar and J. E. Wampler, Occurrence and role of *cis* peptide bonds in protein structures, *J. Mol. Biol.*, 1990, **214**, 253–260, DOI: 10.1016/0022-2836(90)90159-J.

36 T. Drakenberg and S. Forsen, Barrier to internal rotation of amides. I. Formamide, *J. Phys. Chem.*, 1970, **74**, 1–7, DOI: 10.1021/j100696a001.

37 T. Drakenberg and S. Forsén, The barrier to internal rotation in monosubstituted amides, *J. Chem. Soc. D. Chem. Commun.*, 1971, 1404–1405, DOI: 10.1039/c29710001404.

38 R. Jawaria, M. Hussain, Z. Shafiq, H. B. Ahmad, M. N. Tahir, H. A. Shad and M. M. Naseer, Robustness of thioamide dimer synthon, carbon bonding and thioamide–thioamide stacking in ferrocene-based thiosemicarbazones, *CrystEngComm*, 2015, **17**, 2553–2561, DOI: 10.1039/c4ce02566k.

39 M. M. Naseer, M. Hussain, A. Bauzá, K. M. Lo and A. Frontera, Intramolecular noncovalent carbon bonding interaction stabilizes the *cis* conformation in acylhydrazones, *ChemPlusChem*, 2018, **83**, 881–885, DOI: 10.1002/cplu.201800329.

40 J. K. R. Deka, B. Sahariah, K. Baruah, A. K. Bar and B. K. Sarma, Conformational control of *N*-methyl-*N*,*N*′-diacylhydrazines by noncovalent carbon bonding in solution, *Chem. Commun.*, 2020, **56**, 4874–4877, DOI: 10.1039/d0cc00943a.

41 J. J. Roeleveld, S. J. Lekanne Deprez, A. Verhoofstad, A. Frontera, J. I. Van der Vlugt and T. J. Mooibroek, Engineering Crystals Using sp^3-C Centred Tetrel Bonding Interactions, *Chem.–Eur. J.*, 2020, **26**, 10126–10132, DOI: 10.1002/chem.202002613.

42 W. Wang, X. Li, P. P. Zhou and Y. Wang, Catalysis with Supramolecular Carbon-Bonding Interactions, *Angew. Chem.*, 2021, **133**, 22899–22903, DOI: 10.1002/ange.202108973.

43 V. R. Mundlapati, D. K. Sahoo, S. Bhaumik, S. Jena, A. Chandrakar and H. S. Biswal, Noncovalent Carbon-Bonding Interactions in Proteins, *Angew. Chem., Int. Ed.*, 2018, **57**, 16496–16500, DOI: 10.1002/anie.201811171.

44 E. V. Zaryanova, A. A. Ignatov and N. A. Lozynskaya, Synthesis and reactivity of new amide-substituted oxindole derivatives, *Tetrahedron*, 2017, **73**, 6887–6893, DOI: 10.1016/j.tet.2017.10.049.

45 O. Radul, G. Zhungietu, M. Rekhter and S. Bukhanyuk, Simple method for the preparation of 1-substituted isatins, *Chem. Heterocycl. Compd.*, 1983, **19**, 286–288, DOI: 10.1007/bf00513261.

46 S. Gao, J. Zang, Q. Gao, X. Liang, Q. Ding, X. Li, W. Xu, C. J. Chou and Y. Zhang, Design, synthesis and anti-tumor activity study of novel histone deacetylase inhibitors containing isatin-based caps and *o*-phenylenediamine-based zinc binding groups, *Bioorg. Med. Chem.*, 2017, **25**, 2981–2994, DOI: 10.1016/j.bmc.2017.03.036.

47 T. Lu and F. Chen, Multiwfn: A Multifunctional Wavefunction Analyzer, *J. Comput. Chem.*, 2012, **33**, 580–592, DOI: 10.1002/jcc.22885.

48 W. Humphrey, A. Dalke and K. Schulten, VMD: Visual Molecular Dynamics, *J. Mol. Graphics*, 1996, **14**, 33–38, DOI: 10.1016/0263-7855(96)00018-5.

49 A. Frisch, *Gaussian 09W Reference*, 2009, 470, https://gaussian.com/glossary/g09/.

50 M. P. Andersson and P. Uvdal, New scale factors for harmonic vibrational frequencies using the B3LYP density functional method with the triple-ζ basis set 6-311+G (d,p), *J. Phys. Chem. A*, 2005, **109**, 2937–2941, DOI: 10.1021/jp045733a.

51 R. Munir, N. Javid, M. Zia-ur-Rehman, M. Zaheer, R. Huma, A. Roohi and M. M. Athar, Synthesis of novel *N*-acylhydrazones and their CN/NN bond conformational characterization by NMR spectroscopy, *Molecules*, 2021, **26**, 4908, DOI: 10.3390/molecules26164908.

52 A. D. Isravel, J. K. Jeyaraj, S. Thangasamy, W. J. John and D. F. T. NBO, HOMO-LUMO, NCI, stability, Fukui function and hole–electron analyses of tolcapone, *Comput. Theor. Chem.*, 2021, **1202**, 113296, DOI: 10.1016/j.comptc.2021.113296.

53 E. D. Glendening and F. Weinhold, Natural resonance theory: I. general formalism, *J. Comput. Chem.*, 1998, **19**, 593–609, DOI: 10.1002/(SICI)1096-987X(19980430)19:6%3C593::AID-JCC3%3E3.0.CO;2-M.

54 F. Weinhold, C. Landis and E. Glendening, What is NBO analysis and how is it useful?, *Int. Rev. Phys. Chem.*, 2016, **35**, 399–440, DOI: 10.1080/0144235X.2016.1192262.

55 M. Orio, D. A. Pantazis and F. Neese, Density functional theory, *Photosynth. Res.*, 2009, **102**, 443–453, DOI: 10.1007/s11120-009-9404-8.

56 E. Bretschneider and O. Thomas, *Internal Rotation in Molecules*, John Wiley & Sons, London-New-York-Sydney-Toronto, 1974, DOI: 10.1016/0022-2860(75)85024-1.

57 V. Samoshin and N. Zefirov, Conformational transformations of organic-molecules in solutions, *Zh. Vses. Khim. O-va. im. D. I. Mendeleeva*, 1984, **29**, 521–530.

58 J. D. Roberts, Fascination with the conformational analysis of succinic acid, as evaluated by NMR spectroscopy, and why, *Acc. Chem. Res.*, 2006, **39**, 889–896, DOI: 10.1021/ar050229p.

59 O. Tapia and J. Bertrán, *Solvent Effects and Chemical Reactivity*, Springer, Dordrecht, 1st edn, 2006, DOI: 10.1007/0-306-46931-6.

© 2025 The Author(s). Published by the Royal Society of Chemistry